The Combined Signatures of Hypoxia and Cellular Landscape Provides a Prognostic and Therapeutic Biomarker in HBV-Related Hepatocellular Carcinoma

Shipeng Chen*, Yuzhen Gao*, Ying Wang, Toos Daemen

S. Chen* and Y. Gao* contributed equally to this work.

Contents

Figure S1. Selected prognostic TME cells and hypoxia-related genes with their corresponding cells type and gene function.

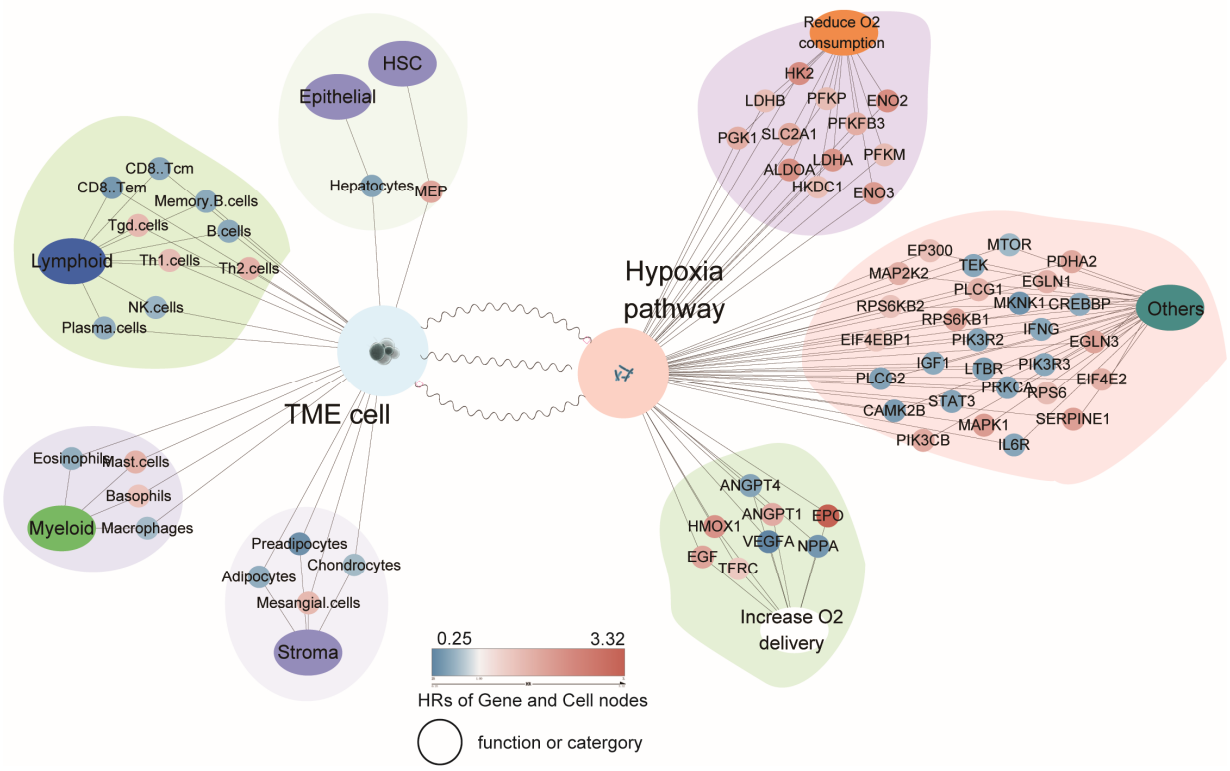

19 prognostic TME cells and 48 hypoxia-related genes were selected based on the meta-analysis from four different HBV-HCC cohorts. The corresponding cells type and gene function were also indicated. Color of each cell/gene node represents the hazard ratio (HR) based on the cox proportional hazards model to the prognosis.

Figure S2. Correlation matrix between hypoxia-related genes and TME cells in tumors of five HBV-HCC cohorts.

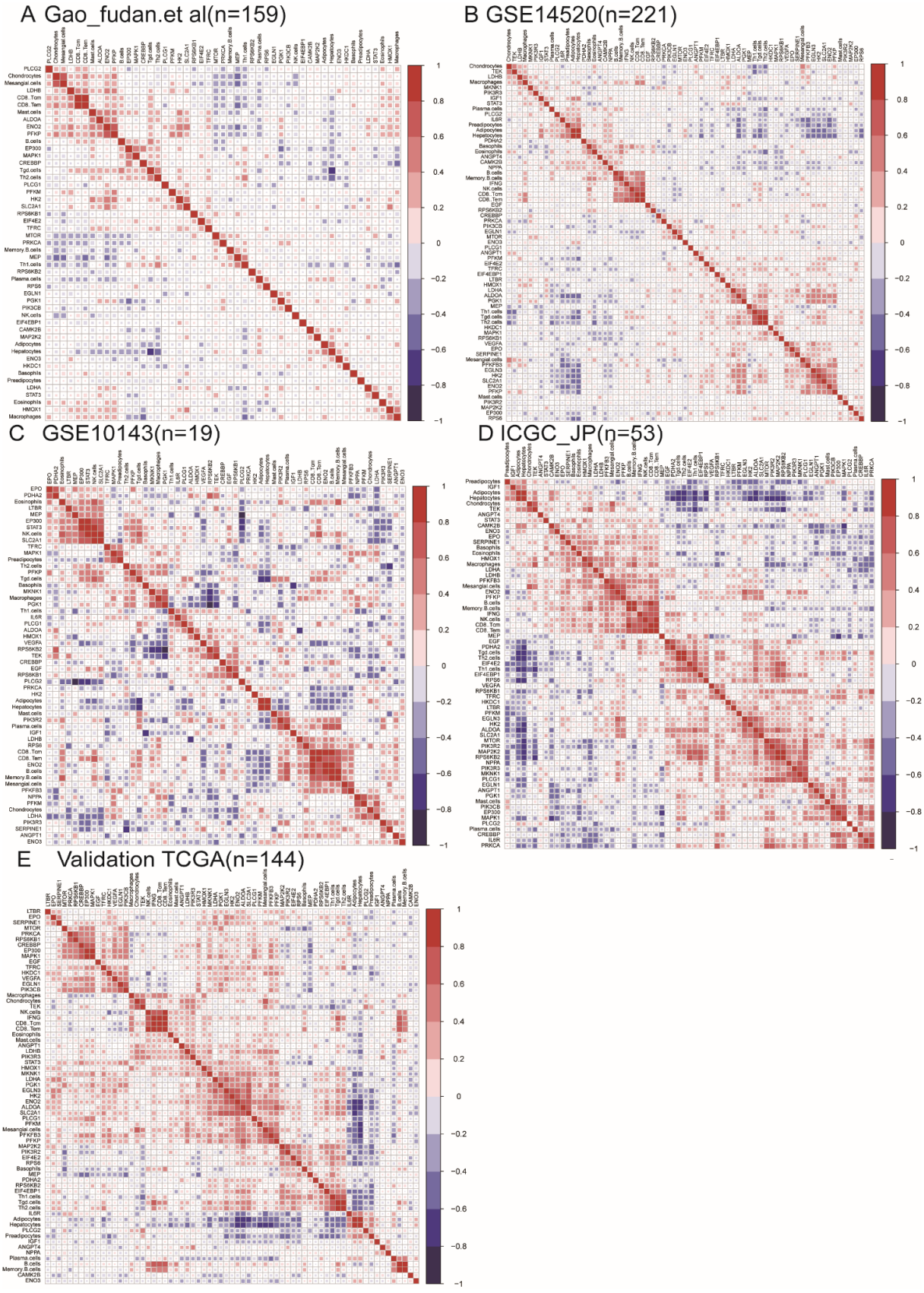

(A-E) Heat map representation of the spearman correlation matrix of the hypoxia-related genes and TME cells in tumors of each cohort. Positive (red) and negative (purple) correlations are indicated.

Figure S3. Gene set enrichment analysis of the HIF-1 signaling pathway in HBV-HCC cohorts.

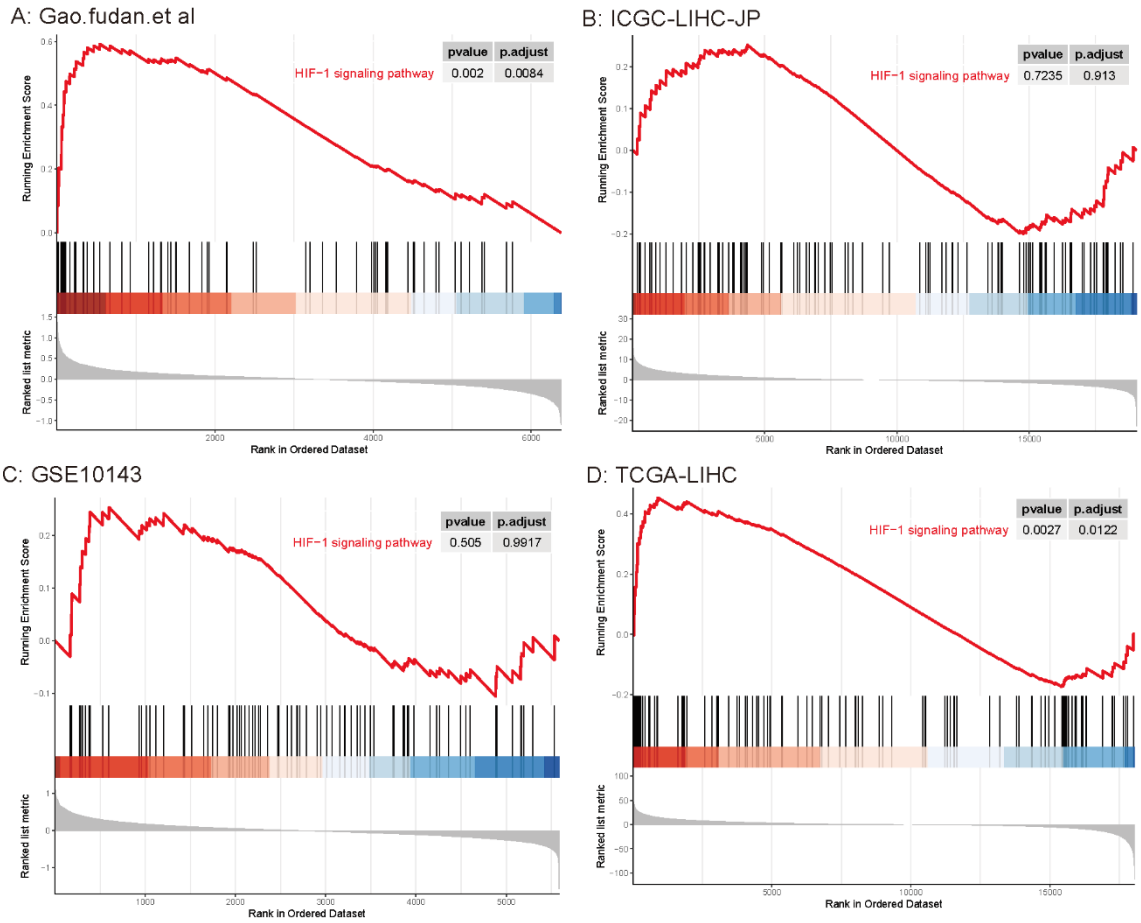

(A-D) Gene Set Enrichment Analysis (GSEA) of 109 genes consist of HIF-1 signaling pathway reveals the association between Hypoxia score and HIF-1 signaling pathway in tumors of each cohort. High hypoxia score located in the left approaching the origin of the x-axis, by contrast, low hypoxia score lay on the right of the x-axis.

Figure S4. Gene set enrichment analysis of the immune response pathway in HBV-HCC cohorts.

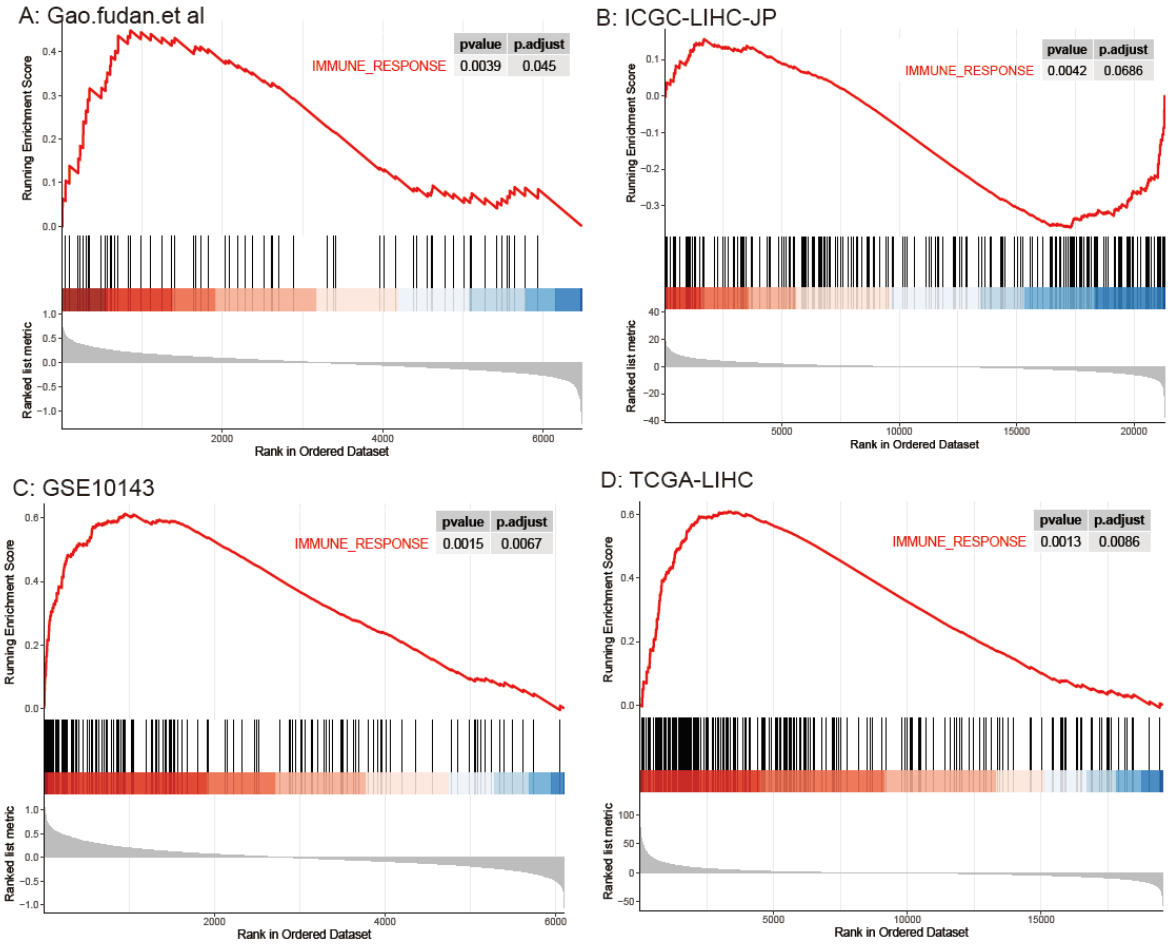

(A-D) Gene Set Enrichment Analysis (GSEA) of 332 genes represent immune response display the association between TME score and immune response in tumors of each cohort. High TME score located in the left approaching the origin of the x-axis, by contrast, low TME score lay on the right of the x-axis.

Figure S5. The correlation between Hypoxia score and TME score in HBV-HCC cohorts and 32 pan-cancer cohorts.

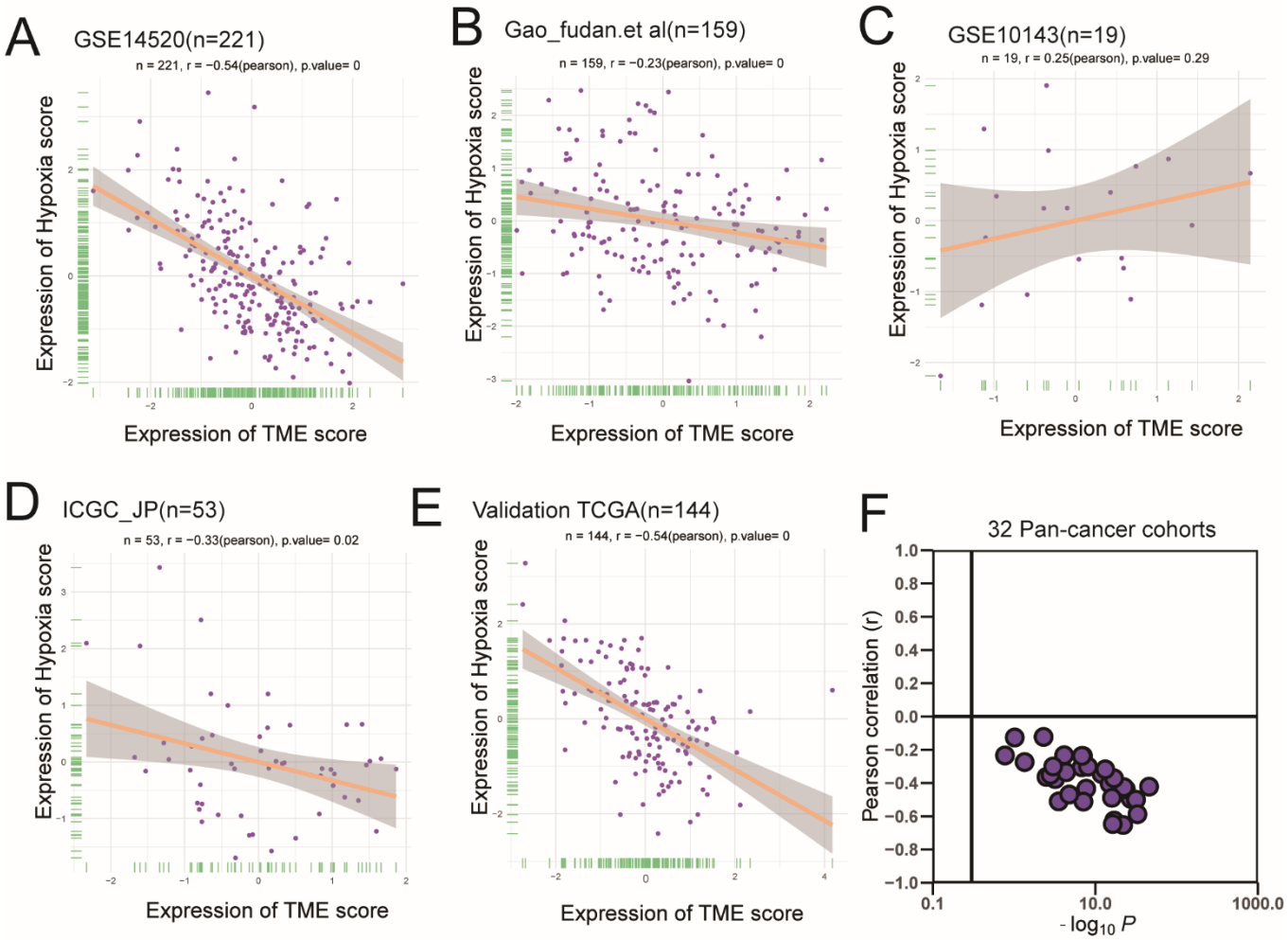

(A-E) The correlation between Hypoxia score and TME score in five HBV-HCC cohorts. The x-axis represents the TME score, and the y-axis represents the Hypoxia score. Each dot represents a tumor sample.

(F) A summarization of the relationship between Hypoxia score and TME score in 32 pan-cancer cohorts. The x-axis represents -$\log_{10}$(P-value), and the y-axis represents Pearson correlation.

Figure S6. The association between Hypoxia-TME classifier and the disease stages in four different HBV-HCC cohorts.

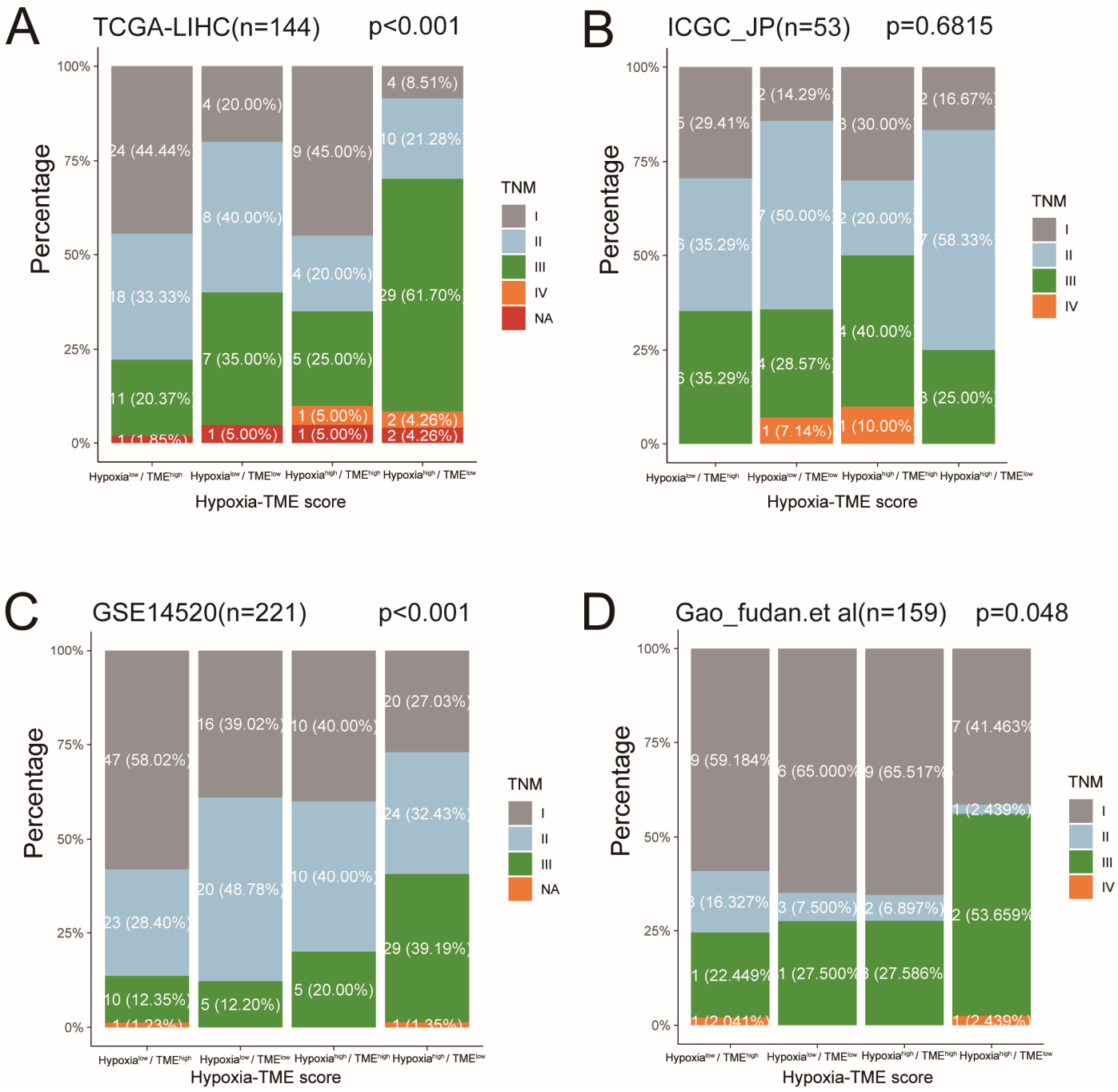

(A-D) The TNM (I-IV) staging has been indicated with different color in these cohorts. NA means tumor staging data was not available.

Figure S7. The prognosis analysis of Hypoxia-TME classifier in HBV-HCC, HCV-HCC, and HCC patients.

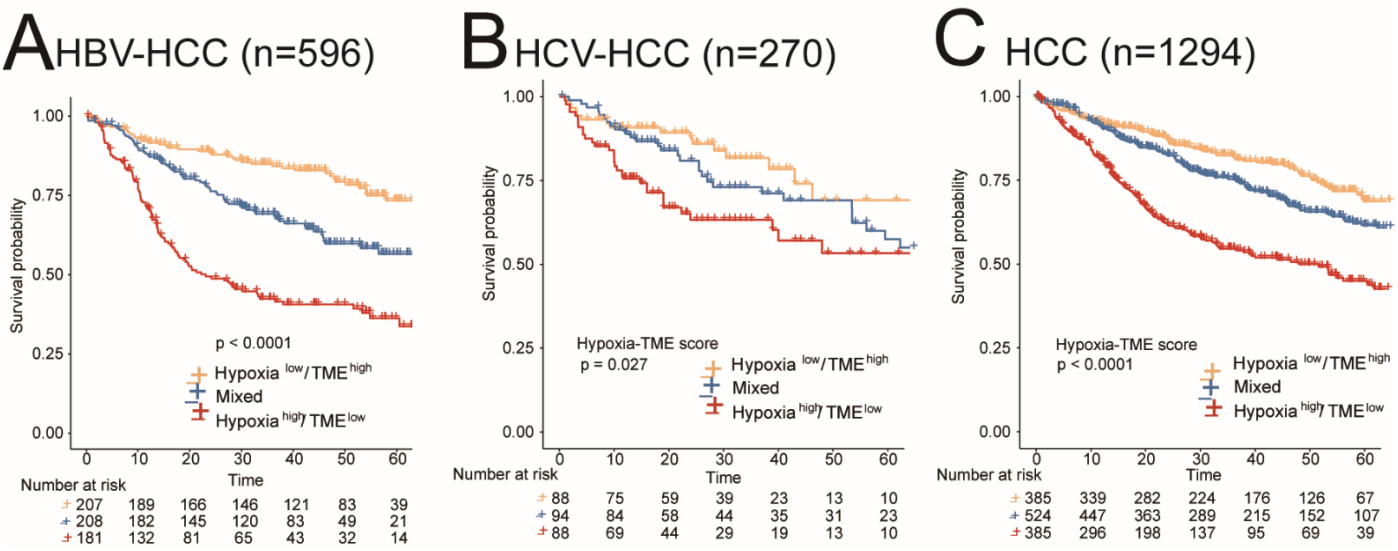

(A-C) Kaplan–Meier overall survival curves of three cohorts which containing HBV-HCC (n=596), HCV-HCC (n=270) and HCC (n=1294), respectively. Each cohort was stratified into three different subgroups based upon the Hypoxia-TME classifier.

Figure S8. Evaluation of the prognostic value of Hypoxia-TME classifier in 32 pan-cancer cohorts.

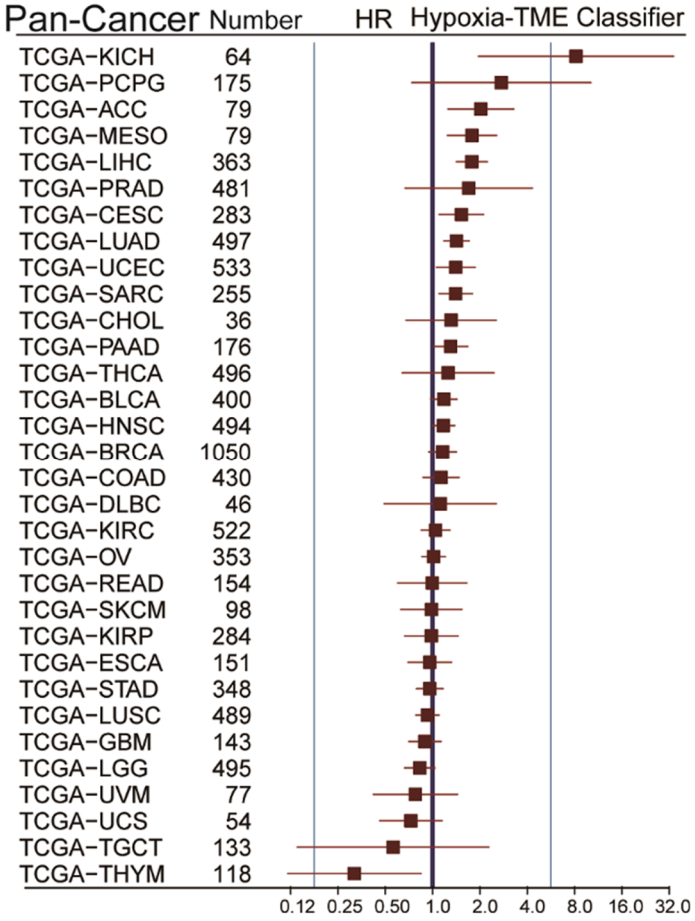

Cox analysis of the Hypoxia-TME classifier in 32 pan-cancer cohorts.

Figure S9. Functional analysis in subgroups of Hypoxia^{low}/TME^{high} and Hypoxia^{high}/TME^{low} illustrated using Proteomaps.

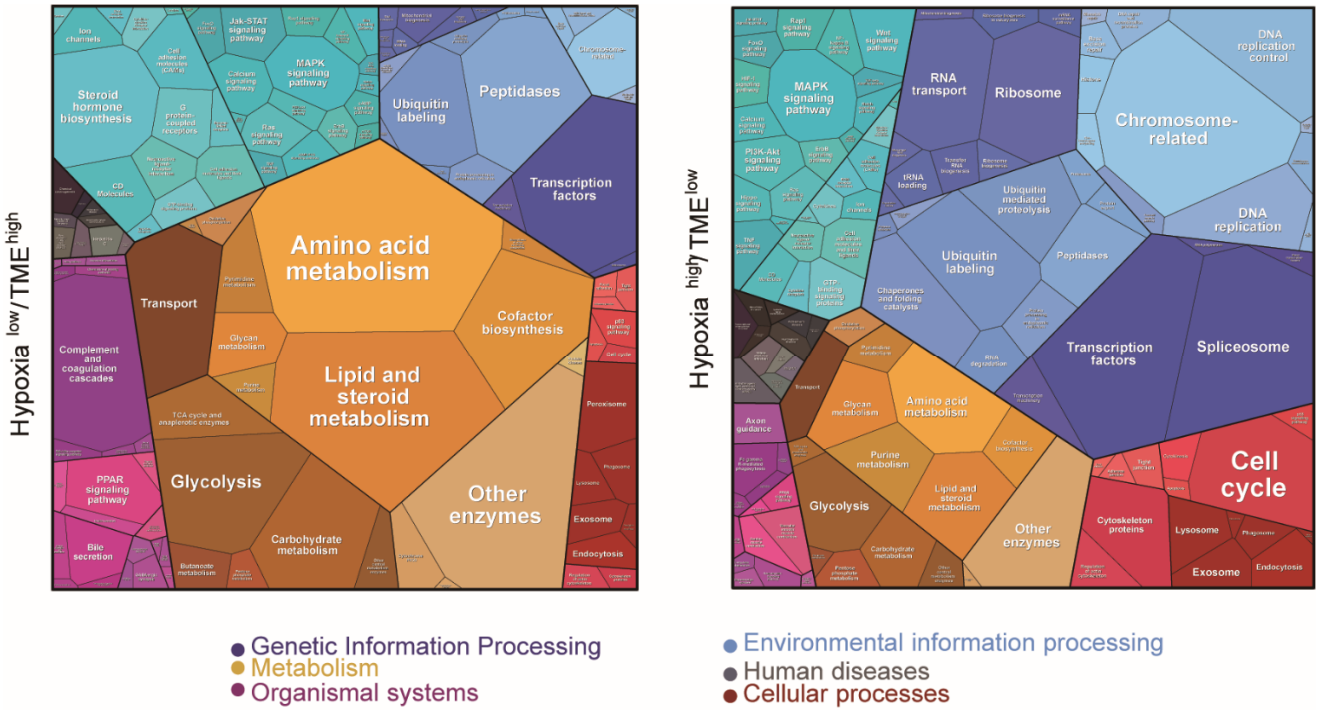

Functional analysis in Hypoxia^{low}/TME^{high} (left) and Hypoxia^{high}/TME^{low} (right), as illustrated using Proteomaps (Liebermeister et al., 2014). Each small polygon corresponds to a single KEGG pathway, and the size correlates with the ratio between the subgroups (GSE14520).

Figure S10. The comparison of immune-related genes in tumors under different Hypoxia-TME subgroups.

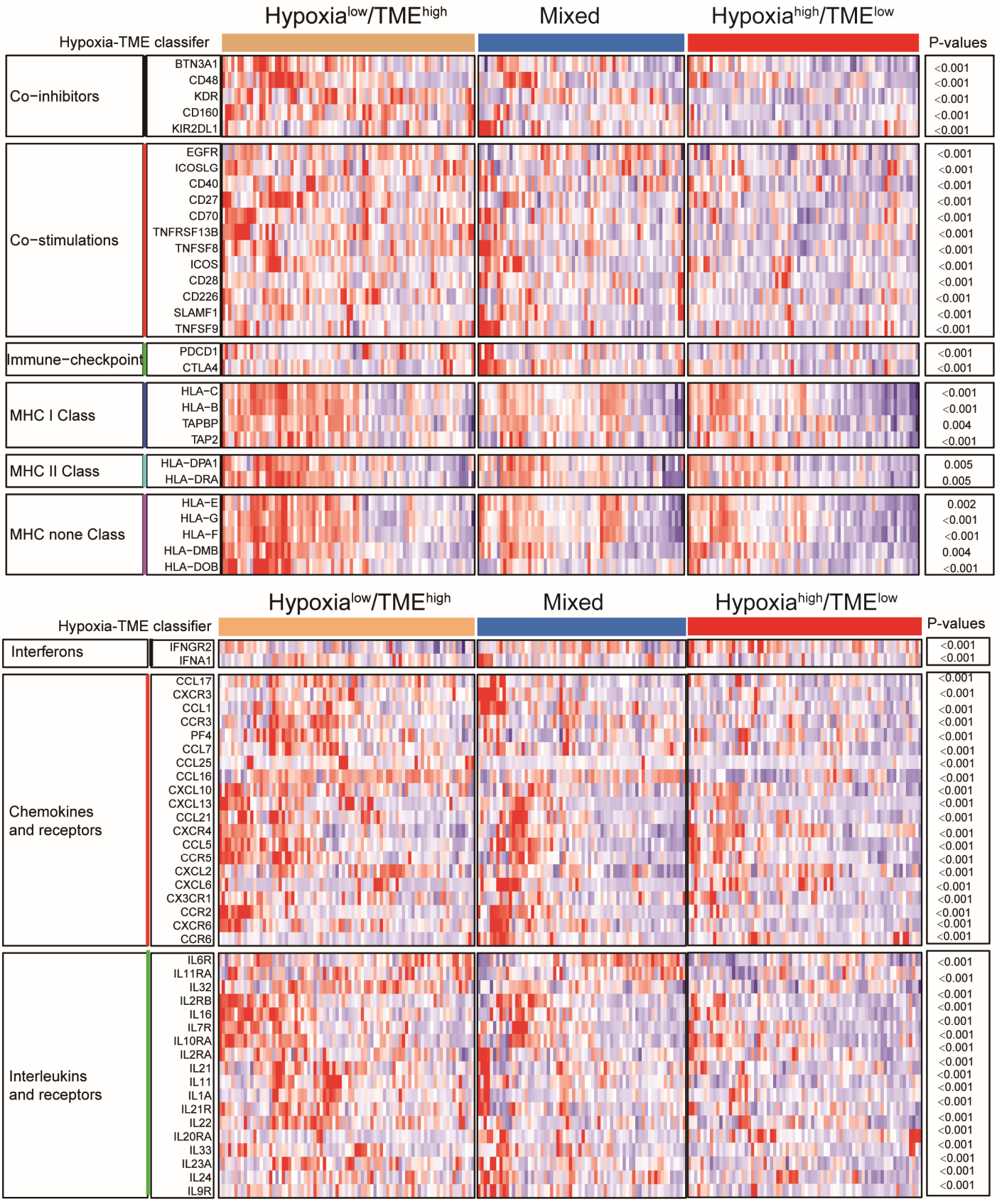

A heatmap for the comparison of immune-related genes under three different Hypoxia-TME subgroups in the GSE14520 cohort.

Figure S11. The difference in tumor somatic mutation among different subgroups based on Hypoxia-TME classifier.

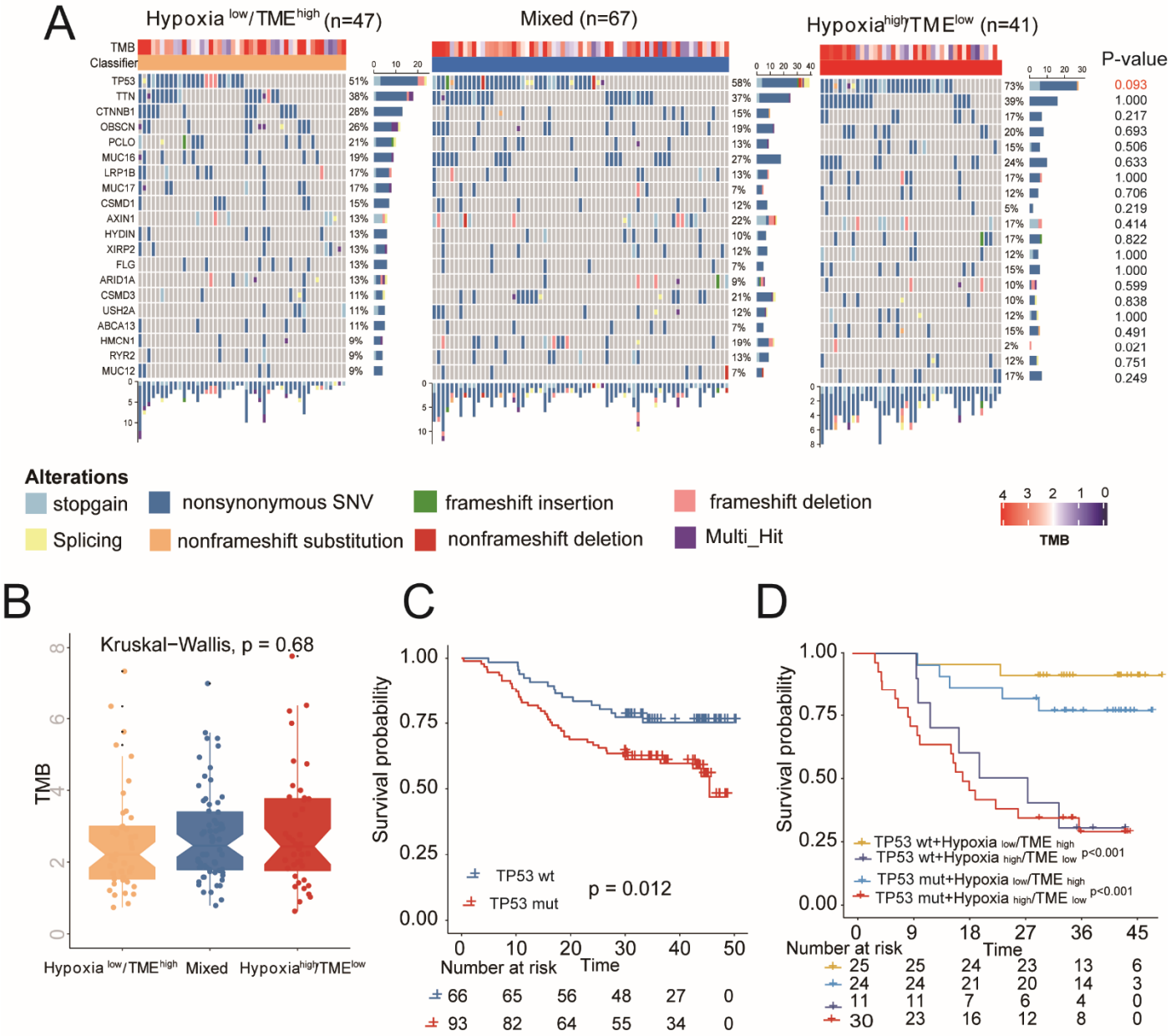

(A) The OncoPrint was constructed by the top 20 mutation genes. Each liver tumor from an individual patient was represented in each column (Gao et al cohort).

(B) Comparison of tumor mutational burden in tumors between defined subgroups by Hypoxia-TME classifier.

(C) Kaplan–Meier overall survival curves of HBV-HCC patients with or without TP53 gene mutation.

(D) Kaplan–Meier overall survival curves of HBV-HCC patients divided by TP53 mutation status and Hypoxia-TME classifier.